Origin of the pH-Dependent Spectroscopic Properties of Pentacoordinate Metmyoglobin Variants[†,‡]

Ralf Bogumil, Robert Maurus, Dean P. Hildebrand, Gary D. Brayer,* and A. Grant Mauk*

Department of Biochemistry and Molecular Biology and the Protein Engineering Network of Centres of Excellence, University of British Columbia, Vancouver, British Columbia V6T 1Z3, Canada

Received December 6, 1994; Revised Manuscript Received April 10, 1995[⊗]

ABSTRACT: The pH dependence of the electronic and EPR spectra of two variants of horse heart myoglobin (Mb) in which the distal His64 ligand has been replaced by either Thr or Ile has been studied. Both of these variants exhibit spectroscopic changes with pH that are indicative of a transition between two ferric high-spin forms that occurs with a pK_a of 9.49 for the His64Thr variant and 9.26 for the His64Ile variant and that is distinctly different from the pH-dependent spectroscopic changes related to titration of the distal aquo ligand of wild-type Mb. The electronic and EPR spectra of both variants at all values of pH studied are consistent with the presence of a pentacoordinate heme iron center. For the His64Thr variant, a high-resolution (1.9 Å) structure determination establishes the lack of the distal aquo ligand and demonstrates an out-of-plane movement of the ferric iron toward the proximal histidine together with a decrease of the Fe−His bond length. Investigation of this pH-linked equilibrium by EPR spectroscopy reveals rhombically split high-spin signals at both pH 7 and 11 with a greater degree of rhombicity exhibited by the alkaline species. We propose that the pH-linked spectroscopic transition exhibited by these distal histidine variants results from the deprotonation of the proximal His93 residue to produce imidazolate ligation at alkaline pH.

The stability of dioxygen binding to ferromyoglobin is controlled in part by formation of a hydrogen bond with the distal histidine (His64, E7) (Philips & Schonborn, 1981; Olson et al., 1988; Rohlfs et al., 1990). Similarly, His64 influences the mechanisms by which various ligands bind to ferrimyoglobin (metMb) [reviewed in Springer et al. (1994)]. In recent years, numerous spectroscopic (Morikis et al., 1990; Egeberg et al., 1990; Rajarathnam et al., 1991; Ikeda-Saito et al., 1992; Balasubramanian et al., 1993; Bogumil et al., 1994; Tang et al., 1994), structural (Quillin et al., 1993; Rizzi et al., 1993; Maurus et al., 1994), and kinetic (Braunstein et al., 1988; Springer et al., 1989; Carver et al., 1990; Cutrozzola et al., 1991; Sakan et al., 1993; Brancaccio et al., 1994) studies of myoglobin variants in which His64 has been replaced with various amino acid residues have clarified the role of the distal histidine in determining the ligand-binding properties of this protein in both oxidation states.

One notable consequence of replacing His64 with other amino acids can be significant alteration in the axial coordination of the ferric heme iron. In wild-type metMb, the presence of the distal histidine results in formation of a hydrogen bond between this residue and a water molecule coordinated to the heme iron atom at the distal coordination position to produce a six-coordinate, high-spin iron center. Substitution of His64 with tyrosine results in His-Fe-Tyr ligation as demonstrated by both spectroscopic and structural analysis (Egeberg et al., 1990; Maurus et al., 1994; Tang et al., 1994; Hargrove et al., 1994). Resonance Raman studies have shown that an arginine at position 64 leads to a six-coordinated, low-spin heme iron, and it has been suggested that the Arg64 in this variant might coordinate to the Fe(III) (Morikis et al., 1990).

On the other hand, several spectroscopic studies have established that the replacement of His64 with nonpolar residues (His64Leu, His64Phe, His64Val) leads to formation of pentacoordinate metMb derivatives that lack the water molecule bound as a sixth ligand at the distal coordination site, while the replacement of His64 with polar residues (His64Gln, His64Asp) permits retention of the coordinated water molecule (Morikis et al., 1990; Ikeda-Saito et al., 1992; Biram et al., 1993; Qin et al., 1993). These findings were recently confirmed by high-resolution X-ray analyses of several His64 variants of sperm whale myoglobin (Mb) (Quillin et al., 1993). The loss of the coordinated water molecule when nonpolar residues are placed at position 64 is primarily attributable to the additional hydrophobicity of the nonpolar residues and to the elimination of the stabilizing hydrogen bond formed by the water and the distal histidine. The substitution of His64 with glycine does not cause loss of the coordinated water because in this case the hydrogen bond with the distal histidine is replaced by a hydrogen bond with a second, well-ordered water molecule (Quillin et al., 1993).

Lack of a water molecule at the distal coordination position is also observed in some naturally occurring globins with hydrophobic residues located at the position corresponding to that of the distal histidine. *Aplysia* Mb (distal His→Val) and *Glycera* hemoglobin (Hb) (distal His→Leu) (Mintoro-

[†] This work and the purchase of the EPR spectrometer, area detector, and computational equipment were supported by the Protein Engineering Network of Centres of Excellence. R.B. is a recipient of a postdoctoral fellowship from the Deutsche Forschungsgemeinschaft (DFG). R.M. is a recipient of an MRC Studentship.

[‡] The atomic coordinates for the structure of the His64Thr variant have been deposited in the Protein Data Bank, Chemistry Department, Brookhaven National Laboratories, Upton, Long Island, NY 11973, under identity code 1HSY.

[⊗] Abstract published in *Advance ACS Abstracts,* July 15, 1995.

0006-2960/95/0434-10483$09.00/0

vitch & Satterlee, 1988; Bolognesi et al., 1989) are examples of such proteins. Interestingly, peroxidases, which possess distal histidyl residues, also appear to be pentacoordinate. Examples of such structures include cytochrome *c* peroxidase (Finzel et al., 1984), lignin peroxidase (Poulos et al., 1993), manganese peroxidase (Edwards et al., 1993), *Coprinus cinereus* peroxidase (Petersen et al., 1994), and *Arthromyces ramosus* peroxidase (Kunishima et al., 1994). Consequently, five-coordinate myoglobin variants that possess a proximal histidyl ligand but no distal ligand may provide useful models for more complex heme enzymes and for defining the structural characteristics that dictate the varied coordination environments that occur in a wide range of heme enzymes.

Detailed spectroscopic analyses involving electronic absorption spectroscopy, EPR, ^{1}H-NMR, magnetic circular dichroism, and X-ray absorption spectroscopy have been reported for the His64Leu, His64Val, and His64Gln variants of human Mb (Ikeda-Saito et al., 1992). In this work, the electronic and EPR spectra of the His64Leu and His64Val variants were observed to differ at pH 6 and 10 despite the fact that these variants are pentacoordinate and, therefore, not expected to undergo the characteristic alkaline transition of wild-type metMb in which the coordinated water molecule is deprotonated at alkaline pH (Antonini & Brunori, 1971). At present, no mechanistic rationale for this behavior of the myoglobin variants has been provided to explain the pH dependence of the spectroscopic properties of these variants.

In the present study, we report an analysis of the pH-dependent spectroscopic properties of the ferric forms of two distal histidine variants (His64Thr, His64Ile) of horse heart Mb involving a combination of electronic absorption spectroscopy and EPR spectroscopy. These results provide a mechanism for the unusual pH dependence of these variants. As part of this work, we also report the high-resolution three-dimensional structure of the His64Thr variant and compare it to that of the wild-type protein and to the structure of the corresponding sperm whale myoglobin variant (Quillin et al., 1993).

EXPERIMENTAL PROCEDURES

Protein Preparation. The expression of a synthetic gene for horse heart myoglobin in *Escherichia coli* has been described by Guillemette et al. (1991), and the variants used in the current study have been reported previously (Bogumil et al., 1994). The preparation and purification of the recombinant horse heart Mb proteins devoid of sulfmyoglobin contamination were performed as described previously (Lloyd & Mauk, 1994).

Electronic Absorption Spectroscopy. Spectra were recorded with a Cary 219 spectrophotometer interfaced to a microcomputer (OLIS, Bogart, GA) and fitted with a thermostated, circulating water bath (Lauda Model RS3). The spectra of the various proteins (25 °C) were recorded (300–700 nm) in 0.1 M potassium phosphate (pH 7) and 0.1 M Ches buffers (pH 10.5). For the spectrophotometric pH titrations, the proteins were exchanged into 0.1 M sodium chloride and the pH was adjusted with microliter quantities of 0.1 M NaOH in a 3 mL quartz cuvette. The p*Ks* for the acid–alkaline transitions were obtained from the absorbance changes at 389 nm (His64Thr) and 395 nm (His64Ile), respectively. The resulting data were analyzed with the program MINSQ (version 4.02, MicroMath, Inc.) and fitted adequately by assuming a one-proton process. The extinction coefficients of the Soret band were determined with the pyridine hemochromogen method (Antonini & Brunori, 1971).

Table 1: Data Collection and Refinement Parameters

Data Collection	
space group	$P2_1$
cell dimensions (Å)	
a	64.4
b	28.9
c	35.8
β (deg)	107.2
no. of measurements	86 121
no. of unique reflections	7270
merging *R*-factor (%)[a]	8.6
Refinement	
no. of reflections used	6916
no. of solvent molecules	53
average thermal factors (Å^2)	
protein atoms	19.9
solvent atoms	31.0
final refinement *R*-factor (%)[b]	16.3

[a] $R_{merge} = \frac{\sum_{hkl}\sum_{i=0}^{n}|I_{i_{hkl}} - \bar{I}_{hkl}|}{\sum_{hkl}\sum_{i=0}^{n} I_{i_{hkl}}}$. [b] $R_{cryst} = \frac{\sum_{hkl}|F_o - F_c|}{\sum_{hkl}|F_o|}$.

EPR Spectroscopy. EPR spectra ([Mb] = 0.7–1 mM) were obtained at X-band frequencies (ca. 9.5 GHz) using a Bruker ESP 300E spectrometer equipped with an Oxford Instruments Model 900 liquid helium cryostat and an Oxford Instruments ITC4 temperature controller. The experimental conditions used were 4 K, microwave power 0.63–2 mW, microwave frequency 9.45 GHz, modulation frequency 100 kHz, and modulation amplitude 0.5–1 mT.

Structure Determination. Crystals of the His64Thr variant were grown at room temperature by the hanging drop vapor diffusion method from a 10 μL droplet containing 8 mg/mL protein, 60–62% ammonium sulfate, 20 mM Tris/HCl, and 1 mM EDTA at pH 8.4, suspended over 1 mL of solution containing 62–65% ammonium sulfate. These crystals were found to be isomorphous with crystals of both wild-type (Evans & Brayer, 1988, 1990) and recombinant wild-type (R. Maurus, C. M. Overall, R. Bogumil, Y. Luo, A. G. Mauk, M. Smith, and G. D. Brayer, manuscript in preparation) horse heart myoglobin (Table 1).

Diffraction data were collected to 1.9 Å resolution from a single crystal of the His64Thr variant with a Rigaku R-Axis II imaging plate area detector system using Cu Kα radiation generated from a RU-300 rotating anode fitted with a monochromator and operated at 90 mA and 59 kV. For each data frame, the crystal was oscillated through a ϕ angle of 1.2° and exposed for 25 min. The crystal to detector distance was set to 78 mm. X-ray intensity data were processed (summarized in Table 1) using R-Axis II software (Higashi, 1990; Sato et al., 1992).

A restrained parameter least squares approach (Hendrickson & Konnert, 1981) was employed to refine the His64Thr variant structure using the 1.7 Å resolution structure of recombinant wild-type horse heart metMb (R. Maurus, C. M. Overall, R. Bogumil, Y. Luo, A. G. Mauk, M. Smith, and G. D. Brayer, manuscript in preparation) as the starting model. Initially, Thr64 was modeled simply as an alanine. Omit and $F_o - F_c$ and $2F_o - F_c$ difference electron density

Table 2: Absorption Maxima (nm) of the Electronic Spectra of Wild-Type and Variant Forms of Horse Heart and Human Myoglobin (Molar absorptivities are indicated in parentheses)[a]

protein	Soret	visible	reference
		Horse Heart Wild-Type	
Fe(III), pH 7	408 (188)	502 (10.2), 630 (3.9)	Antonini and
Fe(III), pH 10.5	412.5 (119)	539 (8.8), 585 (7.8)	Brunori (1971)
Fe(II)	434.5 (121)	560 (13.8)	
Fe(II)CO	424 (207)	540 (15.4), 579 (13.9)	
		Horse Heart His64Thr	
Fe(III), pH 7	395 (109)	506 (13.3), 642 (3.6)	this work
Fe(III), pH 10.5	405 (93)	502 (11.8), 640 (5.7)	
Fe(II)	435 (110)	559 (10.4)	
Fe(II)CO	424.5 (149)	542 (11.3), 574.5 (9.3)	
		Horse Heart His64Ile	
Fe(III), pH 7	394 (100)	506 (12.8), 642 (3.7)	this work
Fe(III), pH 10.5	404.5 (82)	502 (9.7), 640 (5.7)	
Fe(II)	434 (103)	559 (10.8)	
Fe(II)CO	425.5 (161)	542.5 (11.8), 576 (10.2)	
		Human His64Leu	
Fe(III), pH 6.0	395 (103)	507 (nd, 641 (nd)	Ikeda-Saito et al. (1992)
		Human His64Val	
Fe(III), pH 6.0	395 (103)	507 (nd), 641 (nd)	Ikeda-Saito et al. (1992)

[a] Abbreviation: nd, not determined.

maps covering the entire polypeptide chain of the His64Thr variant were examined periodically during refinement. These allowed for the manual adjustment of a number of surface side chain conformations and the placement of the remaining atoms of the Thr64 side chain. Water molecule positions were determined by an iterative procedure (Tong et al., 1994) and retained only if they were found to form reasonable hydrogen bonds to protein atoms as well as refining to a thermal factor <60 Å^2. Final refinement parameters are tabulated in Table 1.

The final refined His64Thr variant structure has excellent stereochemistry with rms bond distance and bond angle deviations from ideality being 0.013 and 0.040 Å, respectively. Atomic coordinate errors have been estimated using two methods. Inspection of a Luzzati (1952) plot indicates an overall coordinate error of 0.18 Å, whereas the corresponding value using Cruickshank's (1985) method is 0.17 Å.

RESULTS

Electronic Absorption Spectra. The absorption maxima and extinction coefficients observed for derivatives of the His64Thr and His64Ile variants are summarized in Table 2. As seen from these data, only small differences are observed between the spectra of the deoxy and CO-bound forms of wild-type Mb and the corresponding forms of the variants. The electronic spectra of recombinant metMb at pH 7 and 10.5 are shown in Figure 1A, and the corresponding spectra of the variants are shown in Figures 1B,C. In contrast to the spectra of the reduced proteins, the spectra observed for the oxidized variants differ considerably from those of the wild-type protein at both neutral and alkaline pH. At pH 7, the Soret bands of the variants are much broader and shifted to higher energy (395 and 394 nm for His64Thr and His64Ile, respectively, versus 408 nm for wild-type Mb). The extinction coefficients of the Soret bands are also significantly lower for both mutants (Table 2). Both of these characteristics are typical of pentacoordinate, high-spin ferriheme proteins (Yonetani & Anni, 1987; Mintorovitch & Satterlee,

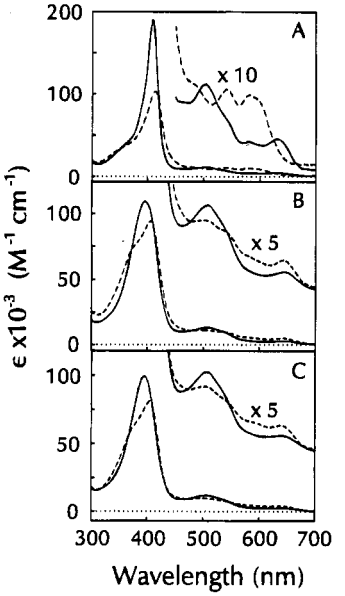

FIGURE 1: Electronic absorption spectra of ferric myoglobins in 0.1 M phosphate (pH 7, solid line) and 0.1 M Ches (pH 10.5, dotted line). (A) Recombinant wild-type (8×10^{-6} M), (B) His64Thr (1.43×10^{-5} M), and (C) His64Ile (1.43×10^{-5} M).

1988; Dunford, 1991; Ikeda-Saito et al., 1992). Significantly, the Soret maximum of the horse heart His64Thr variant (395 nm) differs substantially from that reported for the His64Thr variant of sperm whale Mb (402 nm) (Quillin et al., 1993).

At pH 10.5, the electronic spectrum of wild-type metMb is characteristic of the hydroxo-bound ferriheme derivative[1] with the Soret maximum shifted to lower energy and visible absorption maxima at 539 and 585 nm. The pK for this equilibrium ($H_2O \rightleftarrows OH^-$) is 8.93 (Antonini & Brunori, 1971). In contrast, the spectra of the two distal histidine variants at pH 10.5 are indicative of a five-coordinate ferric high-spin state. The Soret band of His64Thr at pH 10.5 is shifted to 405 nm with a pronounced shoulder (δ band) at ~370 nm and a slight intensification of the visible maximum at ~543 nm. The same effect is observed for the spectrum of the His64Ile variant. A comparable electronic spectrum with a relatively intense δ band is exhibited by cytochrome c peroxidase [λ_{Soret} = 408 nm (ϵ = 98 mM^{-1} cm^{-1}), δ band = 360−380 nm, visible maxima at 505 and 645 nm], a pentacoordinate heme protein with a proximal histidine ligand (Finzel et al., 1984; Yonetani & Anni, 1987). The electronic absorption spectra reported here for the His64Thr and His64Ile variants of horse heart Mb are similar to those reported for the His64Val and His64Leu variants of human Mb at pH 10 (Ikeda-Saito et al., 1992).

The spectrophotometric pH titration of the His64Thr variant of horse heart metMb is shown in Figure 2. The isosbestic points observed for the spectra recorded between pH 7.8 and 10.3 indicate that just two species are responsible for the pH-dependent spectra (Harris & Bertolucci, 1978). The pK_a of this equilibrium obtained by fitting the absorbance change at 389 nm to a one-proton titration (Figure 2, inset) was 9.49 ± 0.04. For the His64Ile variant, a slightly lower pK_a of 9.26 ± 0.04 was obtained. At pH 11 and above, further changes in the absorption spectra are observed that result in a broadening and shift of the Soret band that are

[1] MetMb-OH is more accurately described as a mixture of high- and low-spin components at ambient temperature (Beetlestone & George, 1964; George et al., 1964; Feis et al., 1994).

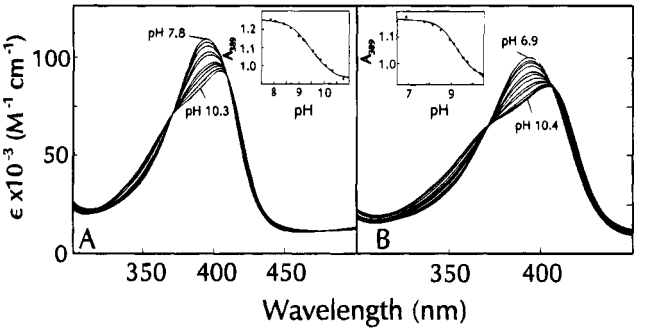

FIGURE 2: pH dependence of the electronic absorption spectrum of the (A) His64Thr and (B) His64Ile variants. In the inset, the absorbances at 389 nm (His64Thr) and 395 nm (His64Ile) are plotted vs pH. The data were fitted to a one-proton titration (continuous line).

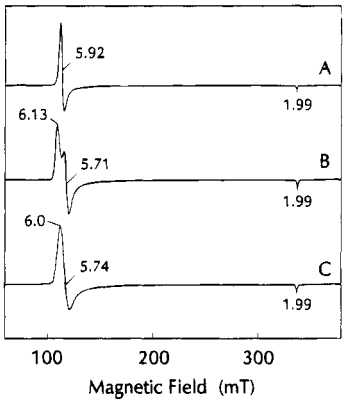

FIGURE 3: X-Band EPR (4 K) spectra of myoglobins at pH 7 (50 mM Hepes). (A) Recombinant wild-type, (B) His64Thr, and (C) His64Ile.

probably attributable to reduced stability and partial denaturation of the protein at high pH.

EPR Spectroscopy. EPR spectra of the wild-type and variant myoglobins were recorded in the pH range 6−11. At pH 7, the wild-type protein exhibits an axially symmetric ferric high-spin signal with g-values of 5.92 and 1.99 (Figure 3). The EPR spectra of the two variants are distinctly different from that of the wild-type protein. For the His64Thr variant, a rhombically split ferric high-spin EPR spectrum is observed with g-values of 6.13, 5.71, and 1.99. While the line shape of the spectrum observed for the His64Ile variant appears to be axially symmetrical, the line width of the signal near $g = 6$ is significantly greater (peak to peak line width of 8.5 mT) than the line width of the axially symmetric EPR spectrum observed for the wild-type protein (peak to peak line width of 3.2 mT). Therefore, the spectrum of His64Ile is better described as slightly rhombic with g-values of 6.0, 5.74, and 1.99 as indicated in Figure 3.

An unexpected buffer dependence was observed in the EPR spectra of distal histidine mutants (His64Val, His64Gln, His64Leu) of human Mb (Ikeda-Saito et al., 1992). Consequently, we also examined the buffer dependence of the EPR spectra at pH 7. Figure 4 shows the expanded region around $g = 6$ of the EPR spectra of His64Thr in Tris, phosphate, and Mes buffers. The spectra in phosphate, Hepes (Figure 3, middle trace), and Mes buffers are quite similar to each other with slight shifts in g-values as summarized in Table 3. In Tris buffer a smaller rhombicity is observed, and the two rhombic components are not as well resolved. For the His64Ile variant, no buffer dependence

Table 3: EPR Parameters for Wild-Type and Variant Forms of Horse Heart Metmyoglobin

protein	g-values
wild-type	
pH 7	5.92, 1.99
pH 10	2.58, 2.17, 1.84
His64Thr	
Hepes (pH 7)	6.13, 5.71, 1.99
Tris (pH 7)	6.03, 5.76, 1.99
phosphate (pH 7)	6.12, 5.73, 1.99
Mes (pH 7)	6.15, 5.70, 1.99
glycine (pH 11)	6.49, 5.47, 1.98
His65Ile	
Hepes (pH 7)	6.0, 5.74, 1.99
Tris (pH 7)	6.0, 5.74, 1.99
Tris (pH 7, 50% glycerol)	6.03, 5.75, 1.99
glycine (pH 11)	6.50, 5.46, 1.98

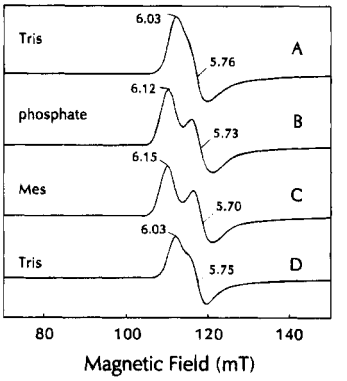

FIGURE 4: Buffer dependence of the EPR spectra (4 K) of Mb variants at pH 7. (A) His64Thr (50 mM Tris), (B) His64Thr (50 mM phosphate), (C) His64Thr (50 mM Mes), and (D) His64Ile (25 mM Tris, 50% glycerol).

of the EPR spectrum was observed. The spectra obtained for samples prepared in Hepes, Mes, phosphate, and Tris buffers at pH 7 are nearly identical to each other with broad signals around $g = 6$. As seen in the case of the His64Ile variant (Figure 4D), slightly greater resolution is achieved in the presence of 50% glycerol. The rhombic character of these spectra (g-values of 6.03 and 5.75) is more apparent than in the spectrum of this variant in the absence of glycerol (Figure 3, bottom trace).

Similar spectra with only slightly rhombic high-spin signals are reported for the His64Leu and His64Val variants of human Mb at pH 7, although a somewhat greater buffer dependence was observed for the human variants (Ikeda-Saito et al., 1992). Generally, spectra obtained for samples prepared in organic buffers such as Hepes and Mes resulted in slightly better resolved spectra of the His64Thr variant as reported for the human Mb variants, although no significant buffer effects were observed for the EPR spectrum of the wild-type proteins. The zwitterionic organic buffers also have the advantage that the pH changes upon freezing are less pronounced than for phosphate or Tris buffers and are, therefore, better suited for cryogenic EPR measurements (William-Smith et al., 1977).

The pH dependence of the EPR spectra observed for the His64Thr variant is shown in Figure 5 (left side). At pH 7 and 11 only one species, a rhombically split high-spin form, is observed. The species present at high pH gives rise to a more rhombic EPR spectrum with g-values of 6.49, 5.47, and 1.98. At pH 10 a mixture of these two forms is observed. A similar pH dependence of the EPR spectra were found for the His64Ile variant (Figure 5, right side). The

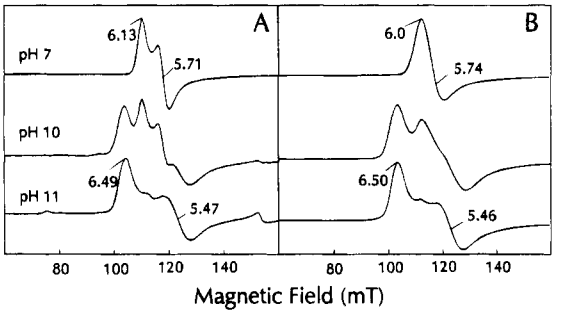

FIGURE 5: pH dependence of the EPR spectra (4 K) of Mb variants. (A) His64Thr and (B) His64Ile: top spectra, pH 7, 50 mM Hepes; middle spectra, pH 10, 50 mM glycine; bottom spectra, pH 11, 50 mM glycine.

g-values of the acid and alkaline forms of the mutants are listed in Table 3. In contrast, the EPR spectrum of wild-type Mb at alkaline pH exhibits a low-spin EPR spectrum resulting from the strong field hydroxo ligand present at high pH (Table 3). No indication of hydroxo-type low-spin EPR signals is found in either of the two variants. The EPR spectra of these variants clearly confirm the existence of an equilibrium between two ferric high-spin species in both variants as observed in the electronic absorption spectra.

For ferric high-spin heme proteins, the percentage of rhombicity can be calculated from the difference in *g*-values (Δg) between the two components near $g = 6$.[2] For the acid form of His64Thr, the percentage of rhombicity is 2.6%, whereas the alkaline species has a rhombicity of 6.4%. The corresponding values for the His64Ile variant are 1.8% and 6.5%, respectively. Significantly, the EPR spectra of the alkaline forms of these variants resemble the EPR spectra of peroxidases, which exhibit rhombically split signal, high-spin EPR signals. For example, the *g*-values observed for cytochrome *c* peroxidase are 6.4, 5.3, and 1.97 (rhombicity 6.9%) (Yonetani & Anni, 1987), while for horseradish peroxidase *g*-values of 6.35, 5.65, and 2.0 (rhombicity 4.3%) are reported (Blumberg et al., 1968).

Structural Studies. The overall conformation of the polypeptide chain of the His64Thr mutant protein was found to be similar to that of wild-type metmyoglobin (Figure 6). The largest discrepancies are observed at the polypeptide chain termini (residue 1 with an average deviation of 0.37 Å and residues 152−153 with an average deviation of 0.56 Å) and residues 42−48. The terminal regions of these proteins are locally disordered and have high thermal parameters. The shifts observed at residues 42−48 represent a displacement of the BC loop region. The average positional deviation of the main chain atoms in this region is 0.33 Å as compared to an overall average of 0.16 Å for all other main chain atoms. Significant side chain positional differences (>0.8 Å) all involve surface-exposed charged residues with the exceptions of Leu61 (average deviation of side chain atoms 0.95 Å) and Ile101 (average deviation of side chain atoms 0.82 Å). The close proximity of Leu61 to residue 64 appears to cause the observed reorientation of the side chain of this residue in the variant. Ile101, on the other hand, is poorly defined in electron density maps for both wild-type and variant proteins, and the observed differences are likely due to positional uncertainty.

[2] Percent rhombicity (%*R*) is defined as $\Delta g/16 \times 100$, where Δg is the absolute difference in *g*-values between the two components near $g = 6$ (Peisach et al., 1971).

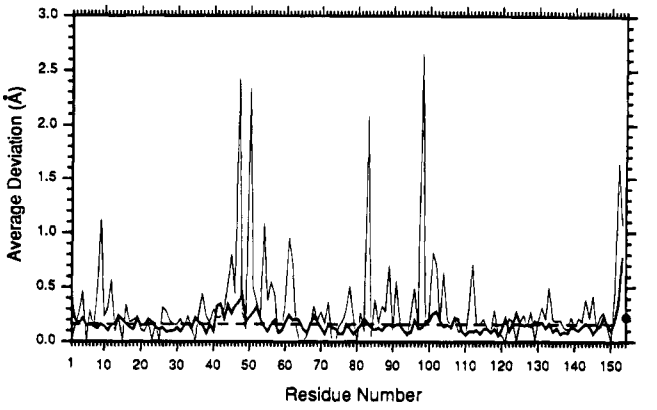

FIGURE 6: Average positional deviations observed in main chain (thick lines) and side chain (thin lines) atoms of the His64Thr variant when compared to wild-type myoglobin. The horizontal dashed line indicates the average positional deviation (0.16 Å) for all main chain atoms. The filled circle at position 154 represents the average positional deviation of the atoms of the heme group.

A detailed comparison of the His64Thr and wild-type structures in the region of the mutation site is shown in Figure 7a. The heme iron is notably drawn out of the porphyrin plane toward the His93 position in the His64Thr variant with the distance between this iron atom and the porphyrin ring plane increasing from the 0.08 Å found in wild-type protein to 0.28 Å (Table 4). The shorter His93−Fe bond that results may contribute to the loss of the distal water molecule which in the wild type protein forms a hydrogen bond to His64. Despite this feature, the conformations of the heme group in the wild-type and His64Thr mutant proteins are comparable, and the observed average deviation in the positions of all 43 atoms is 0.22 Å. This similarity extends to a comparable heme planarity (Table 4) and placements of the proximal heme ligand His93, as well as other residues that constitute the heme binding pocket (Figure 7a). Moreover, the solvent accessibility of the heme group is 31% of the total heme surface (probe sphere radius of 1.4 Å; Connolly, 1983), the same as found for the wild-type structure.

Substantial alterations in the hydrogen-bonding network about the mutation site near the heme in the His64Thr variant are observed. For example, a new hydrogen bond between the side chains of Thr64 and Lys45 is formed (Figure 7). It appears the observed positional shift of residues 42−48 (Figure 6) is related to this newly introduced hydrogen bond. Through a further hydrogen bond in Wat169, which is also present in the wild-type structure, Thr64 also forms a link to Asp60.

DISCUSSION

The spectroscopic and structural studies presented here establish that the coordination environment of the heme iron in the His64Thr and His64Ile distal histidine variants of horse heart metMb is pentacoordinate. While this result was expected to follow from substitution with the large, nonpolar isoleucyl residue (Morikis et al., 1990; Rajarathnam et al., 1992; Ikeda-Saito et al., 1992; Quillin et al., 1993), it contrasts with the recently reported structure of the corresponding His64Thr mutant of sperm whale Mb in which a water molecule (Wat155) was found to be present as the sixth ligand to the heme iron with an occupancy of 72% (Quillin et al., 1993). This water molecule forms a hydrogen bond with the carbonyl oxygen of Thr64 through interaction with a new water molecule, Wat303, that is present in the

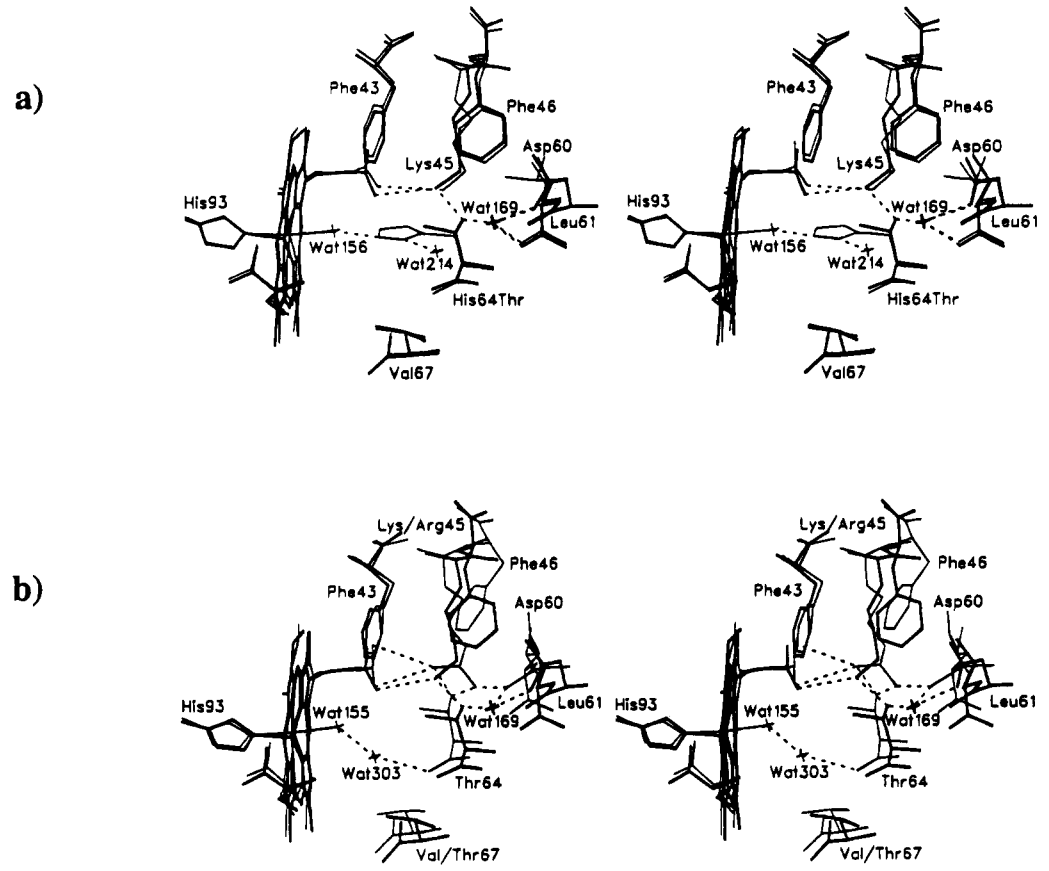

FIGURE 7: (a) Stereodiagram showing the region of the mutation site in the His64Thr variant (thick lines) and wild-type (thin lines) proteins. The conformations of the heme groups are comparable between the two proteins with the exception of the heme iron being drawn out of the porphyrin plane toward His93 in the His64Thr variant. Note the absence of Wat214 and the distal heme ligand Wat156 which in the wild-type protein both form a hydrogen bond to the His64 side chain. The Thr64 side chain in the His64Thr variant hydrogen bonds to Lys45 and also through Wat169 to Asp60. Hydrogen bonds are indicated with dashed lines. (b) Comparison of the region about the His64Thr mutation site in horse heart (thick line) and sperm whale (thin line) myoglobins (Quillin et al., 1993). Significant positional differences are apparent between these two mutant proteins. Sequence differences at positions 45 and 67 are indicated. Neither Wat155 nor Wat303 are observed in horse metmyoglobin. On the other hand, Wat 169 is not observed in sperm whale myoglobin. Hydrogen bonds are indicated with dashed lines.

distal heme pocket of the sperm whale variant protein. Although the overall three-dimensional structures of wild-type sperm whale and horse heart myoglobins are comparable, no coordinated water was found in the current study of the horse heart His64Thr variant (Figure 7).

This difference in distal ligation of the horse heart and sperm whale His64Thr variants appears to result from the combined effects of several relatively subtle differences in the structures of the two proteins. At least four such contributions can be identified. (1) In the horse heart protein, a lysine is present at position 45, while an arginine is present at this position in the sperm whale protein. As a result, the hydrogen-bonding pattern formed by residue 45 with the heme D propionate, Thr64, and Asp60 is different in the two species of protein. Most notably, the NH2 atom of Arg45 in sperm whale Mb is located near the position that Wat169 occupies in the horse heart protein so that Wat169 is not present in the sperm whale protein. (2) The conformation of Phe46 is different in the horse heart and sperm whale variants. In the sperm whale variant, the side chain of Phe46 is located further from the site of axial water coordination than in the horse heart variant. Consequently, no unfavorable interactions between the hydrophilic water molecule and the hydrophobic Phe46 side chain occur in the sperm whale variant. (3) In the horse heart protein, a valine is present at position 67, while a threonine is present at this position in the sperm whale protein. The greater polarity of the threonyl residue would favor the presence of water molecules in the distal heme binding pocket of the sperm whale protein. (4) The position of the backbone carbonyl group of residue 64 in the horse heart Mb is located further from the heme iron than it is in the sperm whale protein, which disfavors the presence of the newly bound water molecule (Wat303) that stabilizes the distal water ligand in the sperm whale protein.

Similarly, at least two differences between the His64Thr horse heart Mb variant and the wild-type protein structures can be identified that contribute to the inequivalent titration behavior of the proximal His ligands in these two proteins. First, in the variant, the ferric high-spin iron moves out of the heme plane (Table 4) and has an Fe−His bond length (1.93 Å) that is shorter than that observed in the wild-type protein (2.12 Å) (R. Maurus, C. M. Overall, R. Bogumil, Y. Luo, A. G. Mauk, M. Smith and G. D. Brayer, manuscript in preparation).[3] This decreased Fe−His bond length could contribute to a decrease in the pK_a of the coordinated imidazole in the variant protein. Second, the *trans* effect of coordination of the anionic hydroxide ligand to the wild-

[3] Note that while the overall estimated coordinate error of the His64Thr variant structure is 0.17−0.18 Å^2, the Cruickshank (1985) method can be used to estimate positional errors for His93NE2 and heme Fe of 0.06 and 0.02 Å, respectively, consistent with the low thermal factors (9.9 and 14.1 Å^2) observed for these atoms. On this basis, we regard the decrease in bond length discussed here to be statistically significant.

Table 4: Heme Geometry of Recombinant Wild-Type and His64Thr Myoglobin[a]

	wild-type	His64Thr
Angular Deviations (deg) of Pyrrole Ring Plane Normals from the Porphyrin Ring Plane Normal		
A	4.25	3.12
B	4.36	2.64
C	3.64	3.47
D	3.04	3.14
Angular Deviations (deg) of Pyrrole Ring Plane Normals from Pyrrole Nitrogen Plane Normal		
A	5.94	1.54
B	4.07	3.47
C	6.62	4.30
D	5.03	4.77
Heme Iron Displacements from the Porphyrin Ring Plane and the Pyrrole Nitrogen Plane (Å)		
porphyrin plane	0.09	0.28
pyrrole nitrogen plane	0.08	0.28
Heme Iron−Ligand Bond Distances (Å)		
His93−NE2	2.12	1.93
Wat156−O	2.17	–
heme−NA	2.03	2.04
heme−NB	2.02	2.01
heme−NC	2.00	1.99
heme−D	1.98	2.00

[a] The pyrrole nitrogen plane is defined by the four pyrrole nitrogen atoms of the heme group. The four pyrrole ring planes are each defined by the five atoms of the ring and the first carbon atom attached to each of the four carbons of the ring. The porphyrin ring is defined by the five atoms in each of the four pyrrole rings, the four bridging methine carbon atoms, the first carbon atom of each of the eight side chains of the heme, and the central iron atom of the heme (33 atoms in total). The heme atom nomenclature used in this table follows the conventions of the Protein Data Bank (Bernstein et al., 1977) and is diagrammatically illustrated in Figure 3 of Berghuis and Brayer (1992).

type protein at alkaline pH should weaken the Fe(III)−His interaction and decrease the effect of metal coordination on the pK_a of the proximal imidazole.

We attribute the pH-dependent electronic and EPR spectra of the His64Thr and His64Ile horse heart metMb variants to an equilibrium between two ferric high-spin forms of the variants that involve deprotonation of the proximal His93 residue to produce imidazolate ligation at alkaline pH with pK_a = 9.49 for the His64Thr variant and pK_a = 9.26 for the His64Ile variant. These values are in the range expected for deprotonation of the proximal histidine and are consistent with the decrease in imidazole pK_a expected to occur upon coordination to a metal ion (Sundberg & Martin, 1974). This behavior is distinctly different from the pH-linked equilibrium of aquo and hydroxo species exhibited by wild-type metMb (Antonini & Brunori, 1971; Feis et al., 1994). Although it would be highly desirable to obtain direct evidence for titration of His92 in these variants by analysis of the variation of their resonance Raman spectra with pH, Morikis et al. (1990) have established that the Fe−His stretching frequency of related variants of sperm whale metMb cannot be observed. Finally, we note that the contribution of any S = 3/2 component to this behavior must be minimal because the EPR spectra exhibit no evidence of such a species by the criteria described by Maltempo (1974) and the NMR spectrum of the His64Ile variant exhibits the broad meso-H resonance at −27 ppm that is characteristic of S = 5/2 systems (D. P. Hildebrand, data not shown).

Several heme proteins and model heme compounds have been reported to exhibit pH-dependent spectroscopic behavior similar to these variants. For example, the electronic spectrum of the heme c group in N^{α}-acetylmicroperoxidase exhibits a pK_a of ~9 that appears to correspond to an equilibrium of two ferric high-spin states (Wang et al., 1992) that has been attributed to the deprotonation of the proximal histidine. Similar behavior has been reported for methemoglobin (Beetlestone & George, 1964; George et al., 1964), ferricytochrome c' (pK_a = 8−9.1, depending on the species; La Mar et al., 1990), and ferricytochrome b_{562} (pK_a = 9.0; Moore et al., 1985). A pK_a of ~10 has been observed for the imidazole complexes of horse heart Mb (Morishima et al., 1980) and *Chironomus* hemoglobin (Mohr et al., 1967), and spectroscopic properties of Fe(III)−heme complexes with coordinated imidazolate have been reported (Quinn et al., 1982; Chacko & La Mar, 1982).

Both variants evaluated in this study exhibit slightly rhombic EPR spectra at neutral pH and significantly increased rhombicity at alkaline pH. This effect is consistent with the greater basicity of an anionic imidazolate ligand. It has been proposed that all pentacoordinate, high-spin ferric heme proteins exhibit rhombically distorted axial symmetric EPR signals and that the degree of rhombicity is related to the degree of interaction with the axial ligand (Yonetani & Anni, 1987). Stronger interaction of this type should increase rhombicity. The EPR spectra of ferric heme proteins with anionic axial ligands (e.g., catalase, cytochrome P-450) exhibit relatively large rhombicity (Palmer, 1979). Highly rhombic EPR spectra are also observed in pentacoordinate Mb variants in which the proximal histidine is replaced by anionic tyrosine or cysteine residues (Adachi et al., 1993; Egeberg et al., 1990). Notably, the EPR and electronic absorption spectra of a horse heart Mb variant in which the proximal histidine is replaced by tyrosine are pH-independent between pH 7 and 10.5 (Hildebrand et al., 1995) consistent with the assignment of the proximal histidine as the titratable group in the variants studied here.

Conversion to a hexacoordinate, low-spin state at high pH also occurs in horseradish peroxidase and the pentacoordinate *Aplysia* Mb. In *Aplysia* Mb, which possesses a proximal histidyl residue, a pK_a of 7.5 is observed that has been suggested to result from binding of a distal hydroxide ligand at high pH (Giacometti et al., 1975). Thus, the pentacoordinate mammalian metMbs that lack a distal His residue seem to be unique in having a pentacoordinate ferric heme center over a wide pH range. Although the EPR and electronic absorption spectra recently reported for the His64Val and His64Leu variants of human Mb (Ikeda-Saito et al., 1992) are similar to those reported here for the related horse heart Mb variants, no explanation was provided for the significant changes observed at alkaline pH. We propose that the deprotonation of the proximal histidine observed for the variants studied here also occurs in the pentacoordinated variants of sperm whale and human Mbs in which large nonpolar residues (Ile, Val, Leu, Phe) have been substituted for the distal histidyl residue (Ikeda-Saito et al., 1992; Travaglini Allocatelli et al., 1993). It may be that the pK_a of this transition is higher in human Mb, which makes the detection of this equilibrium more difficult.

ACKNOWLEDGMENT

We thank Nham Nguyen for skillful technical assistance.

REFERENCES

Adachi, S., Nagano, S., Ishimori, K., Watanabe, Y., Morishima, I., Egawa, T., Kitagawa, T., & Makino, R. (1993) *Biochemistry 32*, 241−252.

Antonini, E., & Brunori, M. (1971) *Hemoglobin and Myoglobin in Their Reactions with Ligands*, North-Holland, Amsterdam, The Netherlands.

Balasubramanian, S., Lambright, D. G., & Boxer, S. G. (1993) *Proc. Natl. Acad. Sci. U.S.A. 90*, 4718−4722.

Beetlestone, J., & George, P. (1964) *Biochemistry 3*, 707−714.

Berghuis, A. M., & Brayer, G. D. (1992) *J. Mol. Biol. 223*, 959−976.

Bernstein, F. C., Koetzle, T. F., Williams, G. J. B., Meyer, E. F., Jr., Brice, M. D., Rodgers, J. R., Kennard, O., Shimanouchi, T., & Tasumi, M. (1977) *J. Mol. Biol. 112*, 535−542.

Biram, D., Garatt, C. J., & Hester, R. E. (1993) *Biochim. Biophys. Acta 1163*, 67−74.

Blumberg, W. E., Peisach, J., Wittenberg, B. A., & Wittenberg, J. B. (1968) *J. Biol. Chem. 243*, 1854−1862.

Bogumil, R., Hunter, C. L., Maurus, R., Tang, H.-L., Lee, H., Lloyd, E., Brayer, G. D., Smith, M., & Mauk, A. G. (1994) *Biochemistry 33*, 7600−7608.

Bolognesi, M., Onesti, S., Gatti, G., Coda, A., Ascenzi, P., & Brunori, M. (1989) *J. Mol. Biol. 205*, 529−544.

Brancaccio, A., Cutruzzola, F., Travaglini Allocatelli, C., Brunori, M., Smerdon, S. J., Wilkinson, A. J., Dou, Y., Keenan, D., Ikeda-Saito, M., Brantley, R. E., Jr., & Olson, J. S. (1994) *J. Biol. Chem. 269*, 13843−13853.

Braunstein, D., Ansari, A., Berendsen, J., Cowen, B. R., Egeberg, K. D., Frauenfelder, H., Hong, M. K., Ormos, P., Sauke, T. B., Scholl, R., Schulte, A., Sligar, S. G., Springer, B. A., Steinbach, P. J., & Young, R. D. (1988) *Proc. Natl. Acad. Sci. U.S.A. 85*, 8497−8501.

Carver, T. E., Rohlfs, R. J., Olson, J. S., Gibson, Q. H., Blackmore, R. S., Springer, B. A., & Sligar, S. G. (1990) *J. Biol. Chem. 265*, 20007−20020.

Chacko, V. P., & La Mar, G. N. (1982) *J. Am. Chem. Soc. 104*, 7002−7007.

Connolly, M. L. (1983) *Science 221*, 709−713.

Cruickshank, D. W. S. (1985) in *International Tables for X-ray Crystallography* (Rasper, J. S., & Lonsdale, J. S., Eds.) 3rd ed., Vol. 2, pp 317−339, D. Reidel Publishing Co., Dordecht, The Netherlands.

Cutruzzola, F., Travaglini Allocatelli, C., Ascenzi, P., Bolognesi, M., Sligar, S. G., & Brunori, M. (1991) *FEBS Lett. 282*, 281−284.

Dunford, H. B. (1991) in *Peroxidases in Chemistry and Biology* (Everse, J., Everse, K. E., & Grisham, Eds.) CRC Press, Inc., Boca Raton, FL.

Edwards, S. L., Raag, R., Wariishi, H., Gold, M. H., & Poulos, T. L. (1993) *Proc. Natl. Acad. Sci. U.S.A. 90*, 750−754.

Egeberg, K. D., Springer, B. A., Martinis, S. A., & Sligar, S. G. (1990) *Biochemistry 29*, 9783−9791.

Evans, S. V., & Brayer, G. D. (1988) *J. Biol. Chem. 263*, 4263−4268.

Evans, S. V., & Brayer, G. D. (1990) *J. Mol. Biol. 213*, 885−897.

Feis, A., Marzocchi, M. P., Paoli, M., & Smulevich, G. (1994) *Biochemistry 33*, 4577−4583.

Finzel, B. C., Poulos, T. L., & Kraut, J. (1984) *J. Biol. Chem. 259*, 13027−13036.

George, P., Beetlestone, J., & Griffith, J. S. (1964) *Rev. Mod. Phys. 36*, 441.

Giacometti, G. M., Da Ros, A., Antonini, E., & Brunori, M. (1975) *Biochemistry 14*, 1584−1588.

Guillemette, G. J., Matsushima-Hibiya, Y., Atkinson, T., & Smith, M. (1991) *Protein Eng. 4*, 585−592.

Hargrove, M. S., Singleton, E. W., Quillin, M. L., Ortiz, L. A., Phillips, G. N., Jr., & Olson, J. S. (1994) *J. Biol. Chem. 269*, 4207−4214.

Harris, D. C., & Bertolucci, M. D. (1978) *Symmetry and Spectroscopy*, Oxford University Press, New York.

Hendrickson, W. A., & Konnert, J. (1981) in *Biomolecular Structure, Function, Conformation and Evolution* (Srinivasan, R., Ed.) Vol. 1, pp 43−57, Pergamon Press, Oxford, U.K.

Higashi, T. (1980) *J. Appl. Crystallogr. 23*, 253−257.

Hildebrand, D. P., Burk, D. L., Maurus, R., Ferrer, J. C., Brayer, G. D., & Mauk, A. G. (1995) *Biochemistry 34*, 1997−2005.

Ikeda-Saito, M., Hori, H., Andersson, L. A., Prince, R. C., Pickering, I. J., George, G. N., Sanders, C. R., Lutz, R. S., McKelvey, E. J., & Mattera, R. (1992) *J. Biol. Chem. 267*, 22843−22852.

Kunishima, N., Fukuyama, K., Matsubara, Hatanaka, H., Shibano, Y., & Amachi, T. (1994) *J. Mol. Biol. 235*, 331−344.

La Mar, G. N., Jackson, J. T., Dugad, L. B., Cusanovich, M. A., & Bartsch, R. G. (1990) *J. Biol. Chem. 265*, 16173−16180.

Lloyd, E., & Mauk, A. G. (1994) *FEBS Lett. 340*, 281−286.

Luzzati, V. (1952) *Acta Crystallogr. 5*, 802−810.

Maltempo, M. M. (1974) *J. Chem. Phys. 61*, 2540−2547.

Maurus, R., Bogumil, R., Luo, Y., Tang, H.-L., Smith, M., Mauk, A. G., & Brayer, G. D. (1994) *J. Biol. Chem. 269*, 12606−12610.

Mintorovitch, J., & Satterlee, J. D. (1988) *Biochemistry 27*, 8045−8050.

Mohr, P., Scheler, W., Schumann, H., & Mueller, K. (1967) *Eur. J. Biochem. 3*, 158−163.

Moore, G. R., Williams, R. J. P., Peterson, J., Thompson, A. J., & Maikins, F. S. (1985) *Biochim. Biophys. Acta 829*, 83−96.

Morikis, D., Champion, P. M., Springer, B. A., Egeberg, K. D., & Sligar, S. G. (1990) *J. Biol. Chem. 265*, 12143−12145.

Morishima, I., Neya, S., & Yonezawa, T. (1980) *Biochim. Biophys. Acta 621*, 218−226.

Olson, J. S., Mathews, A. J., Rohlfs, R. J., Springer, B. A., Egeberg, K. D., Sligar, S. G., Tame, J., Renaud, J.-P., & Nagai, K. (1988) *Nature 336*, 265−266.

Palmer, G. (1979) in *The Porphyrins* (Dolphin, D., Ed.) Vol. IV, pp 313−353, Academic Press, New York.

Peisach, J., Blumberg, W. E., Ogawa, S., Rachmilewitz, E. A., & Oltzik, R. (1971) *J. Biol. Chem. 246*, 3342−3355.

Petersen, J. F. W., Kadziola, A., & Larsen, S. (1994) *FEBS Lett. 339*, 291−296.

Phillips, S. E. V., & Schoenborn, B. P. (1981) *Nature 292*, 81−82.

Poulos, T. L., Edwards, S. L., Wariishi, H., & Gold, M. H. (1993) *J. Biol. Chem. 268*, 4429−4440.

Qin, J., La Mar, G. N., Cutruzzola, F., Allocatelli, C. T., Brancaccio, A., & Brunori, M. (1993) *Biophys. J. 65*, 2178−2190.

Quillin, M. L., Arduini, R. M., Olson, J. S., & Phillips, G. N., Jr. (1993) *J. Mol. Biol. 234*, 140−155.

Quinn, R., Nappa, M., & Valentine, J. S. (1982) *J. Am. Chem. Soc. 104*, 2588−2595.

Rajarathnam, K., La Mar, G. N., Chiu, M. L., Sligar, S. G., Singh, J. P., & Smith, K. M. (1991) *J. Am. Chem. Soc. 113*, 7886−7892.

Rizzi, M., Bolognesi, M., Coda, Alessandro, Cutruzzola, F., Travaglini Allocatelli, C., Brancaccio, A., & Brunori, M. (1993) *FEBS Lett. 320*, 13−16.

Rohlfs, R. J., Mathew, A. J., Carver, T. E., Olson, J. S., Springer, B. A., Egeberg, K. D., & Sligar, S. G. (1990) *J. Biol. Chem. 265*, 3168−3176.

Sakan, Y., Ogura, T., Kitagawa, T., Fraunfelter, F. A., Mattera, R., & Ikeda-Saito, M. (1993) *Biochemistry 32*, 5815−5824.

Sato, M., Yamamoto, M., Imada, K., Katsube, Y., Tanaka, N., & Higashi, T. (1992) *J. Appl. Crystallogr. 25*, 348−357.

Springer, B. A., Egeberg, K. D., Sligar, S. G., Rohlfs, R. J., Mathews, A. J., & Olson, J. S. (1989) *J. Biol. Chem. 264*, 3057−3060.

Springer, B. A., Sligar, S. G., Olson, J. S., & Phillips, G. N., Jr. (1994) *Chem. Rev. 94*, 699−714.

Sundberg, R. J., & Martin, R. B. (1974) *Chem. Rev. 74*, 471−517.

Tang, H.-L., Chance, B., Mauk, A. G., Powers, L., Reddy, K. S., & Smith, M. (1994) *Biochem. Biophys. Acta 1206*, 90−96.

Tong, H., Berghuis, A. M., Chen, J., Luo, Y., Guss, M., Freeman, H., & Brayer, G. D. (1994) *J. Appl. Crystallogr. 27*, 421−426.

Travaglini Allocatelli, C., Cutruzzola, F., Brancaccio, A., Brunori, M., Qin, J., & La Mar, G. N. (1993) *Biochemistry 32*, 6041−6049.

Wang, J.-S., Tsai, A.-L., Heldt, J., Palmer, G., & Van Wart, H. E. (1992) *J. Biol. Chem. 267*, 15310−15318.

Williams-Smith, D. L., Bray, R. C., Barber, M. J., Tsopanakis, D., & Vincent, S. P. (1977) *Biochem. J. 167*, 593−600.

Yonetani, T., & Anni, H. (1987) *J. Biol. Chem. 262*, 9547−9554.

BI9428080